Modeling of Nanoparticles Formation by Mixing of Two Reactive Microemulsions

A. Ramesh Kumar, G. Hota, A. Mehra, and Kartic C. Khilar
Dept. of Chemical Engineering, Indian Institute of Technology, Bombay, Powai, Mumbai 400076, India

DOI 10.1002/aic.10137
Published online in Wiley InterScience (www.interscience.wiley.com).

A stochastic population balance model for the formation of nanoparticles, involving mixing of two micellized aqueous solutions containing the individual reactants, respectively, has been developed to study the effects of various parameters that influence the formation process of nanoparticles. Population balance equations have been formulated assuming a cooperative mode of intermicellar exchange in an attempt to explore the largest possible particles that can form in a given system. The proposed model essentially divides the entire population of micelles into different categories and formulates the equations describing the rate of change of the probabilities of different states of the micelles in each category. The effect of parameters, such as nucleation rate, intermicellar exchange rate, critical nucleation number, and concentration of the reactants on the particle sizes that can be obtained, has been investigated. The model predictions show a reasonable qualitative agreement with experimental data. © 2004 American Institute of Chemical Engineers *AIChE J,* 50: 1556–1567, 2004
Keywords: nanoparticles, population balance, intermicellar exchange, critical nucleation number, nucleation rate

Introduction

Nanoparticles with controlled properties are of scientific as well as technological interest. Many properties change drastically if crystallite sizes fall below the submicron range (Gleiter, 2000). Nanoparticles have a high specific surface area, interfacially dominated properties, and electrical/optical properties that can be distinguished with respect to corresponding bulk materials on the one hand and individual molecules on the other. Therefore, nanoparticles find applications in diverse fields such as catalysis, microelectronic devices, optical devices, pharmaceuticals, paints, ceramics, semiconductors, advanced biomedical applications, and nanotechnology. To meet the primary specifications of these applications, a precise control over the particle sizes and particle size distributions (PSDs) is necessary, during their preparation.

One way of preparing these nanoparticles is to precipitate them in swollen reverse micelles, which act as nanoreactors. Reverse micelles or water-in-oil microemulsions have attracted much attention as potential reaction media for the preparation of highly monodisperse nanoparticles. A wide variety of physical and chemical methods have been developed for the preparation of nanoparticles, and precipitation in reverse micelles has been shown to be an ideal method for the control of particle size and PSDs. The surfactant stabilized nanocavities provide a cagelike environment that serves to limit the particle nucleation, growth, and agglomeration at a nanoscale.

Reverse micelles have been used to produce nanoparticles of pure metals like copper (Pileni et al., 1997); silver; silver halides (Bagwe and Khilar, 1997; Hirai et al., 1996; Pileni et al., 1997); semiconductor materials like CdS, ZnS, PbS, and Ag2S (Hirai et al., 1994; Lianos and Thomas, 1987; Motte, 1996; Petit et al., 1990; Suzuki et al., 1996); metal oxides like ZnO and TiO_2 (Hingorani et al., 1993; Hirai et al., 1993; Wang et al., 1999), silica (Chang et al., 1996; Esquena et al., 1997); and MoS_3 (Boakye et al., 1994). These studies report the effects of various parameters like water-to-surfactant molar ratio and the reactant concentrations on particle sizes and

Correspondence concerning this article should be addressed to K. C. Khilar at kartic@che.iitb.ac.in.

PSDs. However, data on the effects of dynamic properties of the microemulsion, such as intermicellar exchange rate on particle sizes and PSDs, are scarce (Bagwe and Khilar, 1997, 2000).

The synthesis of nanoparticles by reverse micelles is viable and attractive because not only does it produce nanoparticles that have a narrow size distribution but also the particle sizes can be easily controlled by varying the microemulsion composition. The reaction may be conducted in two modes:

(1) The gas-liquid mode, in which one of the reactants is passed as a gas through the microemulsion containing the other reactant (Kandori et al., 1988; Sato et al., 1997). In this case, the gas dissolves in the continuous phase (oil) and diffuses into the (aqueous) micellar core where the reaction takes place, resulting in the formation of the product species.

(2) The liquid–liquid mode, where the synthesis may be further classified into two types, the simple addition type, where the reducing or precipitating reagent is directly added to the microemulsion containing the other reactant (Motte, 1996), and a multiple microemulsion method, where two or more microemulsions, each containing a reactant, are mixed together.

The micelles undergo numerous collisions and thereby the reactants are exchanged, mixed, and react to form the product. Nanoparticles of different materials, described above, have been prepared using this technique. The particles produced by the simple addition method can be much larger than the original droplet size but in the latter method the sizes are much smaller than the original droplet size (Li and Park, 1999). This work deals with the two microemulsions mixing method.

In the microemulsions mixing method, the two reactants are premicellized in two separate microemulsions and are brought into contact through intermicellar exchange to conduct the reaction. In some cases, where reaction rates are very rapid, the overall reaction rate is governed by the intermicellar exchange rate (Hatton et al., 1993). Unlike in gas–liquid systems, here the fusion–fission and exchange of contents between colliding micelles leads to reaction and also disrupts the initially established Poisson distribution of the reactant in the micelles. The intermicellar exchange rate plays a significant role in the nanoparticle formation and the effect has been studied (Bagwe and Khilar 1997, 2000). Different research groups have obtained trends for the effect of intermicellar exchange rate (Bagwe and Khilar, 1997), water-to-surfactant molar ratio (Bagwe and Khilar, 1997; Monnoyer et al., 1995), and concentration of reactants (Monnoyer et al., 1995). Some controversies exist in the literature on the effect of these parameters on the terminal particle sizes. For instance, different research groups have reported qualitatively different findings on the effect of water-to-surfactant molar ratio on the terminal particle size (Bagwe and Khilar, 1997; Monnoyer et al., 1995; Motte et al., 1996).

Although the formation process involves diffusion, collision, exchange, reaction, nucleation, and growth of nuclei, timescale analysis of these processes leads to different models. One of the early attempts was by Nagy (1989), who provided a very simplified analysis of precipitation process in the case of the single-microemulsion method, by assuming that all the reaction and nucleation are completed initially and the remaining nonnucleated micelles contribute to the growth of the already formed nuclei. Natarajan et al. (1996) extended this model by considering fusion–fission mechanisms for the intermicellar exchange process, which leads to nuclei formation in micelles having atoms greater than the critical nucleation number and also subsequent growth of the nucleus. Reaction, nucleation, and growth were assumed to be instantaneous processes. Bandyopadhyaya et al. (1997) developed a model to describe the formation of $CaCO_3$ nanoparticles considering finite rates for nucleation and diffusion of gas into a micelle.

In the case of two microemulsions mixing method, various mechanisms for intermicellar exchange have been proposed (Barzykin et al., 1994; Bommarius et al., 1994; Fletcher et al., 1987). Because the process of nanoparticles formation is stochastic in nature, Monte Carlo simulation is probably a natural choice; however, it is computationally intensive given that the number of micelles to be considered in a simulation can be very large. A mean field approximation with Monte Carlo simulation is probably needed to account for all the possible combinations of various species in the micelles and outcomes of the fusion–fission events. The population balance equations with mean field approximation, restricting the maximum number of molecules in a micelle, can be solved and the PSDs can be computed from the fraction of nucleated micelles.

There are three possible modes of solute redistribution that may occur upon the fusion–fission of colliding micelles, within the cores of reverse micelles: random, cooperative, and repulsive (Hatton et al., 1993). In random distribution the probability of a molecule to be incorporated into the reverse micellar core does not depend on the number of solubilized molecules already present (Barzykin and Tachiya, 1993). The cooperative mode of solubilization assumes an enhanced probability for a solute to move into a micelle already containing the solubilizates. This, for instance, leads to a simplifying assumption that in a fusion–fission process, the entire solute will be transferred into one micelle and leave one micelle empty. In repulsive distribution this tendency is reduced. However, a range of redistribution scenarios may be possible on the basis of the manner in which the solute enters and leaves the micelles.

In general, although a significant amount of experimental work has been done to study the effect of synthesis variables, modeling studies—concerned with particle formation and the effect of intermicellar dynamics along with synthesis variables—are limited to only a few publications. In the present work the population balance model developed by Natarajan et al. (1996) has been extended to describe the two microemulsions mixing technique and the effects of the important parameters affecting particle size distributions have been investigated. Specifically, we have examined the effects of water-to-surfactant molar ratio, intermicellar exchange rate, nucleation rate, and autocatalysis aspects.

Model formulation

The system considered here is the bimolecular reaction between A and B, which produces C. The reactants are solubilized in two separate microemulsions, which are then mixed together. The Brownian motion of the micelles leads to intermicellar collisions and sufficiently energetic collisions lead to a mixing of micellar contents. Reaction occurs when micelles containing A and B undergo such fusion, which is followed by fission of the fused mass back to two micelles

$$A(l) + B(l) \xrightarrow{\text{Instantaneous reaction}} C(l) \xrightarrow{\text{Finite nucleation rate}} C\,(\text{solid}) \downarrow \tag{1}$$

Assumptions

The following major assumptions are made in this model.

(1) Initially, the reactant species are distributed in reverse micelles according to the Poisson distribution (Natarajan et al., 1996).

(2) The collisions are assumed to be attributed to Brownian motion of micelles and only binary collisions are important.

(3) Reaction and the particle growth in a micelle are assumed to be instantaneous. Therefore, the coexistence of A and B salt molecules in the same micelle is not allowed. Nucleation and intermicellar exchange are assumed to proceed with a finite rate. Further, the number of nucleation events in a micelle is limited to one, and the transfer of nucleus to another micelle containing a nucleus (during the fusion process) does not occur. Therefore, one micelle can contain only one particle.

(4) Nucleation is assumed to occur when the number of product molecules in a micelle exceeds the critical nucleation number.

(5) Cooperative mode of solubilization and autocatalysis effect have been considered for the fusion–fission step to explore the largest particle sizes that can be generated from the model. The autocatalysis effect implies that when one of the micelles is carrying a particle, the reaction always proceeds on that particle. When both are nucleated, reaction takes place in the micelle containing the bigger particle (larger area; Quintillan et al., 2001). The cooperative mode of exchange is likely to produce more empty micelles and fewer large particles with the narrowest size distribution. Experimental observations also follow this trend.

Initial distribution of reactant molecules

The initial distribution of salt molecules among the reverse micelles is assumed to be described by Poissonian statistics. The average occupancy number, which is the number of salt molecules per micelle, z_{avg}, is calculated as

$$z_{avg} = \frac{C_s V_{aq}}{\dfrac{(S - \text{CRMC}) V_{org}}{N_{agg}}} \tag{2}$$

where *CRMC* is the critical reverse micellar concentration and N_{agg} is the aggregation number of reverse micelle. The initial Poissonian distribution of salt molecules is given by

$$p_z = \frac{(z_{avg})^z e^{-z_{avg}}}{z!} \tag{3}$$

where z ranges from 0 to z_{max}, and can be independently set, based on physical arguments. The total reverse micelle concentration, M_{tot}, and the volume of the reverse micelle aqueous core, V_{mic}, are calculated as (Natarajan et al., 1996)

Table 1. Notations Used for States of Micelles

No.	Micelle Class	Content
1	a	A salt molecules
2	b	B salt molecules
3	za	Product molecules and A salt molecules
4	zb	Product molecules and B salt molecules
5	pa	Particle and A salt molecules
6	pb	Particle and B salt molecules
7	p0	Empty

$$M_{tot} = \frac{(S - \text{CRMC})}{N_{agg}} \tag{4}$$

$$V_{mic} = \frac{V_{aq}}{M_{tot} N_A V_{org}} \tag{5}$$

Fusion–fission rules

(1) The collision between two nonnucleated (nonempty) micelles results in transfer of entire solute in one micelle and the formation of an empty micelle.

(2) The fusion between two micelles containing different reactants in each results in complete mixing of the solutes followed by reaction in one micelle and the formation of an empty micelle.

(3) The fusion between a nucleated and a nonnucleated (nonempty) micelle results in transfer of entire solute into the micelle containing a nucleus, leading to growth of the existing nucleus and the formation of an empty micelle.

(4) The collision of any micelle with an empty micelle results in no change.

(5) The autocatalysis effect has been considered for collisions involving nucleated micelles.

Population Balance Equations

The entire population of micelles is divided into seven classes, shown in Table 1. Population balance equations describing the rate of change of probabilities of all possible states of these micelles have been formulated based on the above mentioned fusion–fission rules. The complete set of population balance equations is given in the Appendix. Every population balance equation is of the form

$$\frac{dpx(k)}{dt} = R_1 - R_2 \tag{6}$$

where R_1 and R_2 are the rates of generation and loss of state k in the micelle class x by the various mechanisms of nucleation, intermicellar exchange, and so forth.

Parameter estimation

Nucleation Rate. The theory of homogeneous nucleation is considered for application to nucleus formation in the micelles in view of their small size and the absence of impurities. The nucleation rate k_i in a nonnucleated micelle containing i product species ($i > n^*$) is given by (Adamson 1990; Bandyopadhya et al., 1997)

$$k_i = \begin{cases} 0 & \text{if } i < n^* \\ iA \exp\left[-\dfrac{16\pi\sigma^3 V_{met}^2}{3(k_B T)^2 (\ln \lambda)^2} \right] & \text{if } i \geq n^* \end{cases} \quad (7)$$

where A is the preexponential factor, σ is the interfacial tension between the particle and water, V_m is the volume of one metal atom, λ is the supersaturation calculated based on the solubility product of the product species and number of product molecules in the micelle, and n^* is the critical nucleation number.

Intermicellar Exchange Rate Coefficient. The rate of exchange E of the material between micelles may be written as

$$E = \text{collision frequency } (\text{s}^{-1}\,\text{m}^{-3}) \times \text{efficiency of fusion of micelles} \times \text{matter exchanged in one fusion–fission event}$$

Further, the Brownian collision frequency between equisized micelles is given by (Smoluchowski, 1916)

$$q_m = \frac{8k_B T}{3\eta} \quad (8)$$

so that

$$E = \frac{8k_B T N_b^2}{3\eta} e\left(\frac{1}{2N_A}\right) \sum_{i=1}^{z_{\max}} \sum_{j=1}^{z_{\max}} P(n_i) P(n_j) \times |\text{number of moles of species exchanged}| \quad (9)$$

The term within the double summation sign, is representative of the number of moles of species exchanged in a collision averaged over a large number of collisions. The factor 1/2 arises because every micelle has been counted twice. The term within the modulus is dependent on the mode (cooperative, random, repulsive, etc.) adopted for the exchange. From the definition of a second-order exchange rate coefficient, k_{ex},

$$E = k_{ex} C_{s1} C_{s2} \quad (10)$$

where, C_{s1} and C_{s2} are the aqueous phase concentrations of the two reactant species; in terms of number of atoms and molecules, z_{avg}, that a micelle holds, we have

$$C_{s1} = (z_{avg1} N_{b1})/N_A \quad (11)$$

Combining Eqs. 9, 10, and 11, we obtain

$$k_{ex} = \frac{4k_B T e}{3\eta N_A z_{avg1} z_{avg2}} \sum_{i=1}^{z_{\max}} \sum_{j=1}^{z_{\max}} P(n_i) P(n_j) \times |\text{number of moles of species exchanged}| \quad (12)$$

In the present model the second-order exchange rate coefficient k_{ex} is converted into a first-order rate coefficient, as reported by Natarajan et al. (1996) and represented as

$$\alpha = k_{ex} \times M_{tot} \quad (13)$$

Particle Size. Nanoparticles are assumed to be spherical and a packing fraction, ϕ, for the product molecules inside a micelle has been used to calculate the average particle diameter. Thus,

$$d_p = \left[\frac{6 z V_{met}}{\pi \phi} \right]^{1/3} \quad (14)$$

where V_{met} is the volume of one product molecule. The number-average particle size, $\langle d_p \rangle$, has been calculated from the population of nucleated micelles, by the definition

$$\langle d_p \rangle = \frac{\sum_{i=n^*}^{z_{\max}} \sum_{j=0}^{z_{\max}-i} [ppa(i)(j) \times d_p + ppb(i)(j) \times d_p]}{\sum_{i=n^*}^{z_{\max}} \sum_{j=0}^{z_{\max}-i} [ppa(i)(j) + ppb(i)(j)]} \quad (15)$$

where d_p is the particle size calculated for $z = i$ from Eq. 14.

The population balance equations formulated here are nonlinear, first-order ordinary differential equations, which have been solved using a Runge–Kutta 4th-order solver. The number of equations depends on the value of z_{max}, which is chosen such that the computational results are independent of this value.

Results and Discussion

Comparison with experimental data from the literature

A significant amount of experimental work has been done to study the effect of water-to-surfactant molar ratio, concentration of reactants, and intermicellar exchange rate on the particle size and particle size distributions.

Ultrafine CdS nanoparticles were prepared by Hirai et al. (1994) and they studied the effects of water-to-surfactant molar ratio and the concentration of the reactants, on particle size variation with time, primarily to examine the coagulation phenomenon that occurs after the completion of particle formation by exchange, nucleation, and growth. The particle-formation process, from 10 ms to 3600 s, was followed by monitoring the change in UV-absorption. After a time period ranging from 0.02 to 0.1 s (depending on the reactant concentrations), they observed that the absorbance peak remained constant, indicating the completion of reaction, nucleation, and particle growth. The increase in particle size after this time was assumed to occur as a result of coagulation. The proposed model, in this study, predicts the particle size variation only up to the completion of nucleation and particle growth. The comparison of time variation of particle sizes as obtained experimentally and those predicted by the model is shown, for different concentrations of the reactants, in Figure 1. The experimental conditions were maintained at $R = 6$, [AOT] = 0.1 kmol/m^3 and the concentrations of the reactants were varied to study the effect. The simulation parameters used were taken from Ueda and Schelly (1988) and are indicated in the figure itself.

Comparison with experimental data from the present work

Preparation of CdS Nanoparticles and Comparison with the Model Predictions. One of the most widely studied systems experimentally is the formation of CdS nanoparticles. There-

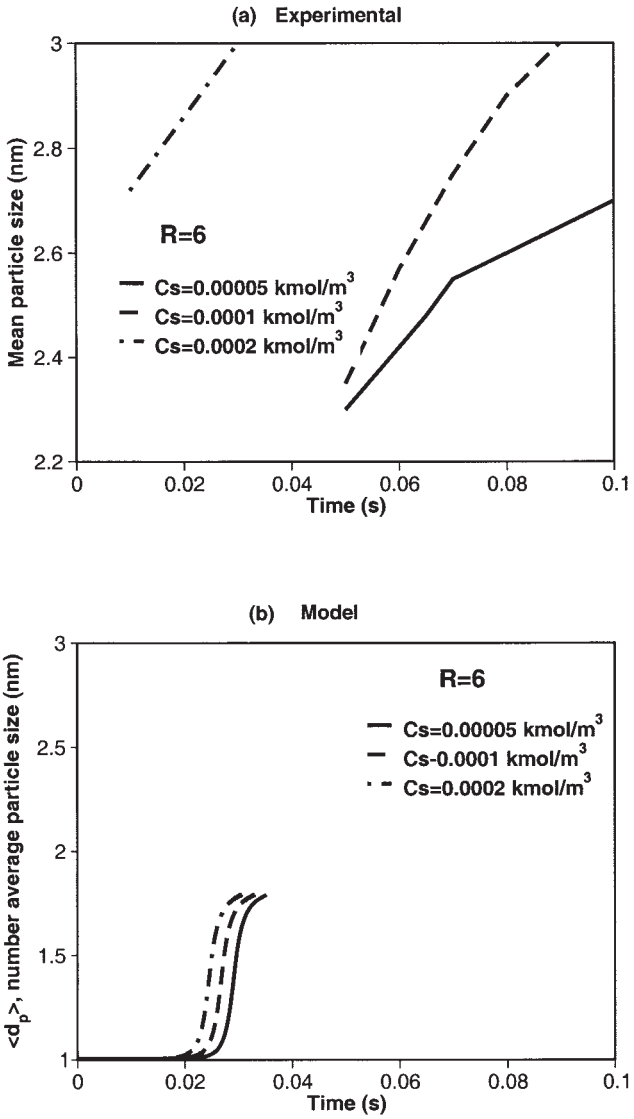

Figure 1. Comparison of model predictions with experimental investigations of Hirai et al. (1994), for CdS nanoparticles prepared in AOT/ isooctane/water microemulsions.

(a) Experimental data; (b) model predictions.

fore, it was thought desirable to augment the available data by further experiments on the CdS system.

A typical Cd^{+2}-containing microemulsion was prepared by solubilizing 0.045 cm^3 of 0.1 kmol/m^3 $Cd(NO_3)_2$ solution in 2.5 cm^3 of 0.1 kmol/m^3 AOT/heptane stock solution; the second microemulsion containing sulfide ion was prepared by solubilizing 0.045 cm^3 of 0.1 kmol/m^3 aqueous $(NH_4)_2S$ solution in 2.5 cm^3 of AOT stock solution (for the case of $R = 10$). Formation of CdS nanoparticles could be observed visually (yellow coloration) after mixing the two microemulsions. UV–vis absorption spectroscopy was used to obtain the average particle size. The absorption spectra were recorded using a Shimadzu UV–visible spectrophotometer (UV-165, Shimadzu, Kyoto, Japan). The microemulsions containing precipitated nanoparticles were used directly for absorption studies. Standard blank microemulsions (without reactants) were used as reference. A Philips 200 CM, HR-TEM instrument (Philips, Eindhoven, The Netherlands) was used to characterize the particle size. The maximum resolution of the instrument was 0.2 nm. TEM samples were prepared by placing a drop of microemulsion, containing the particles, directly onto carbon-coated copper grids. After 600 s the grid was dipped in a sufficient amount of *n*-heptane to remove all the surfactant and then dried for 1 h under IR lamp before taking the images. Figure 2 shows the TEM micrograph of CdS nanoparticles and it can be seen that the particles are not in spherical shape and the size is approximately 3.0 nm, which agrees well with that obtained from UV–vis data. The experimental data, compared with the model computations and comparison, are shown in Figure 3. We observe from this figure that both the data and model prediction show that the terminal particle size is weakly influenced by the water-to-surfactant molar ratio, even though the experimentally observed sizes are greater than the computed values.

From the comparisons presented here, it is reasonable to conclude that the experimentally observed variation of terminal particle size with concentration, water-to-surfactant molar ratio, and so forth are qualitatively well predicted by the model. An observation, common to the two sets of data presented above, is that the experimentally observed sizes are larger than those given by the model computations, even though these are of the order of the diameter of the micellar core. Although this issue is not so severe for the experimental data shown in figures, the average size values reported by some investigators (see Table 2) are much larger than the size of the micellar core. Here, the number of product molecule (z) that needs to be "packed" inside a micelle, to give the experimentally derived sizes, can be much greater than what the micelle can actually contain, given the intrinsic core volume.

Consider the following sample calculation: a particle equal to the micellar core diameter of 3.5 nm, using Eq. 14, yields a value about 240 product molecules to be present (z) [data used: $\phi = 0.7$, $V_{met} = 0.006545$ nm^3]. If the particle size were 10 nm then, by the use of the same equation, the number of product molecules "packed" into the micelle is

$$\frac{z\ (\text{at } 10\text{ nm})}{z\ (\text{at } 3.5\text{ nm})} = \left[\frac{10}{3.5}\right]^3 = 23$$

times more (that is, about 6000 molecules). This raises two interesting issues: (1) how large a particle can actually be "inside" of a micelle; and (2) there are probably mechanisms beyond the reaction, nucleation, and growth—included in the proposed model—that account for the large particle sizes observed experimentally.

Model predictions and discussion

The effect of important parameters on the terminal particle sizes and particle size distributions, such as intermicellar exchange rate, critical nucleation number, concentration of the reactants, and initial reactant ion ratio were computed from the model for the CdS nanoparticle formation in the AOT/ isooctane/water system. Some new insights have been gained from the simulation results, particularly on the effects of the

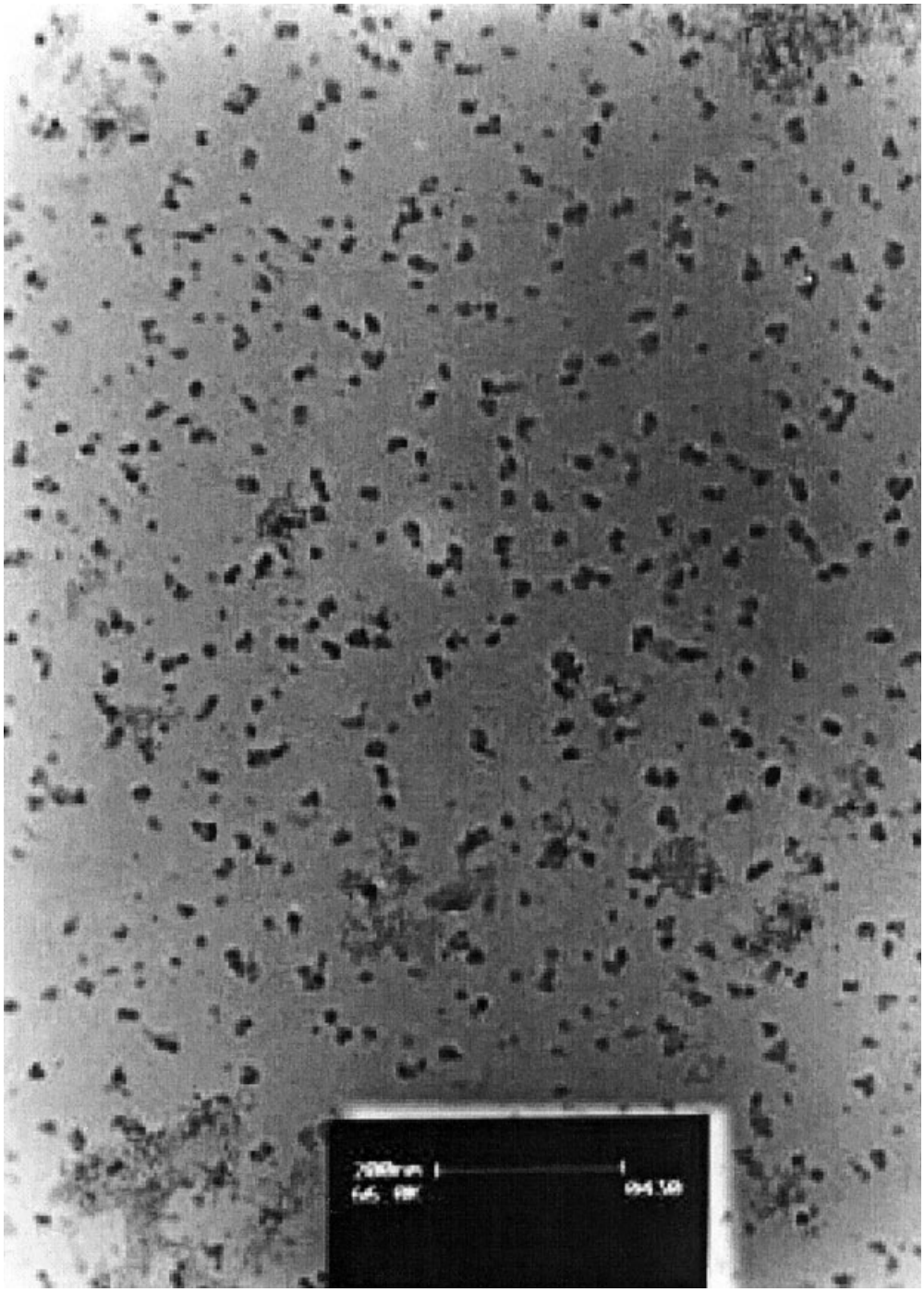

Figure 2. TEM micrograph of CdS nanoparticles prepared in AOT/*n*-heptane/water microemulsion for $R = 10$.

intermicellar exchange rate. The base or reference data for the CdS nanoparticle system have been used as input for the simulations. In all subsequent figures, k_i ranges from 50 to 750 s^{-1}, as computed from Eq. 7, for the relevant range of i values (n^* to z_{max}).

Effect of Intermicellar Exchange Rate. The effect of intermicellar exchange rate on the particle size for different water-to-surfactant molar ratios is shown in Figure 4. It is observed that, in general, the effect of intermicellar exchange rate on terminal particle size at high exchange rates is very weak. At low exchange rates, however, the terminal particle size shows a variation with increasing exchange rates. The terminal particle size increases with exchange rate at $R = 5$, whereas it decreases for $R = 15$. At a high value of R, the average occupancy (salt molecules/micelle) is high, implying that there will be micelles having an occupancy number greater than the critical number for nucleation. At low exchange rates, whatever reaction product forms goes to form nuclei rather than be picked up for growth of an existing particle in another micelle. Thus we have a large number of nuclei of small sizes. Up to

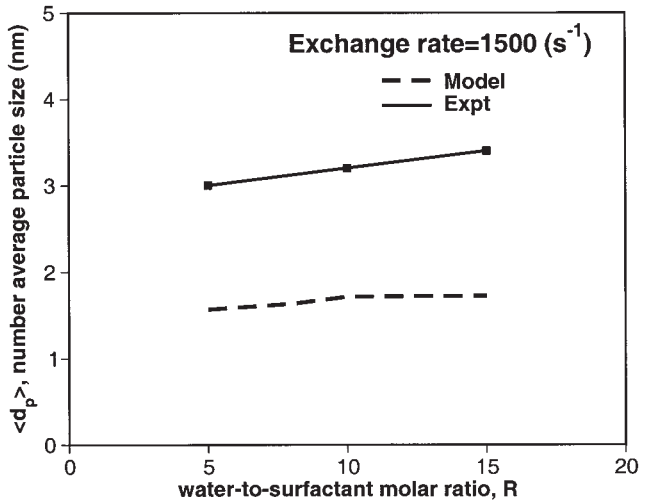

Figure 3. Comparison of model predictions with experimental data for CdS nanoparticles prepared in AOT/*n*-heptane/water microemulsions.

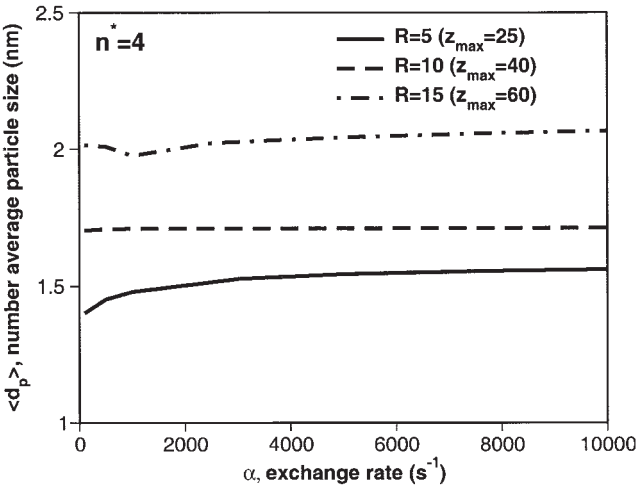

Figure 4. Effect of exchange rate on the number-average particle size for different values of water-to-surfactant molar ratio.

some point, with increasing exchange rate, reaction and nucleation are promoted to greater extents rather than particle growth resulting in decreasing particle sizes. In the case of low values of R, the number of nucleation events are lower, leading to a large number of micelles with number of metal atoms less than the critical number that are thus available for the growth of existing nuclei rather than formation of fresh nuclei. Here, the product molecules tend to be mopped up for growth of existing particles before they nucleate. This leads to fewer and large particles. As the exchange rate increases this tendency toward growth is promoted, leading to fewer and larger particles.

It is interesting to note that the particle-size distributions shown in Figure 5 are dependent on the exchange rates as well as the average occupancy (water-to-surfactant molar ratio). At low R, when the exchange rates are small we obtain a "normal" distribution. As the exchange rate increases, at exchange rates higher than 3000 s^{-1}, the particle-size distribution is entirely skewed toward right, thus forming larger particles. At high R, the exchange rate has a weak influence on the particle size distribution and one obtains large numbers of small and large particles with lesser number of medium sized particles.

Effect of Concentration of Reactants A and B. The effect of concentration of the reactants on the terminal particle size as well as the particle size distributions is shown in Figure 6. At low concentrations (low occupancies) the micelles with molecules greater than critical nucleation number will be low and hence fewer numbers of nuclei are formed; freshly forming product contributes to growth, thereby increasing the particle

Table 2. Typical Experimental Values of Particle Sizes and Ion Occupancies Reported in the Literature

Reference	Maximum Particle Size (nm)	Average Occupancy
Pileni, 1997	13	<1
Bagwe and Khilar, 1997	10.1	7.97
Monnoyer et al., 1995	12	7
Lianos and Thomas, 1986	10	1.5

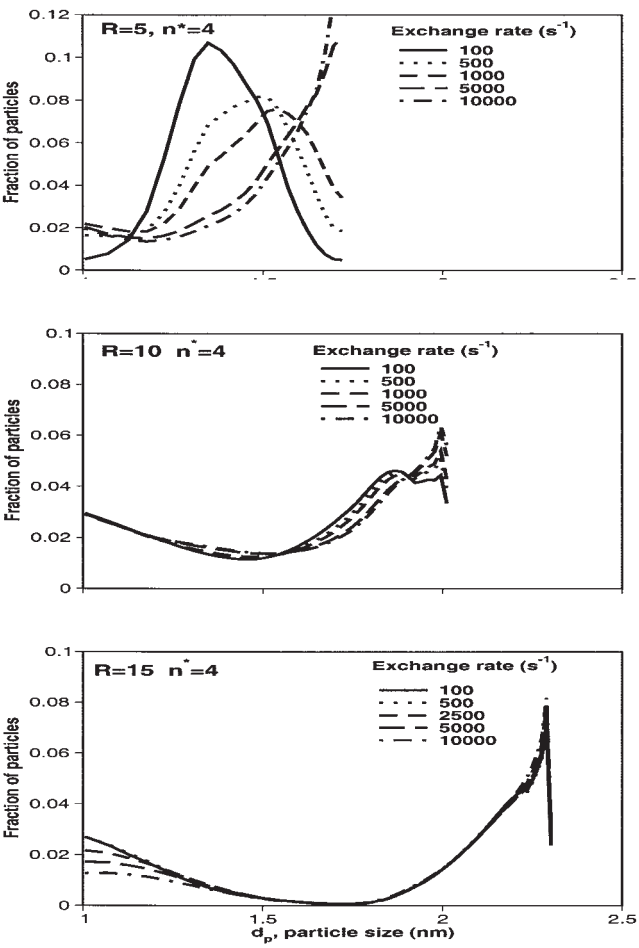

Figure 5. Effect of exchange rate on the particle-size distributions for different values of water-to surfactant molar ratio.

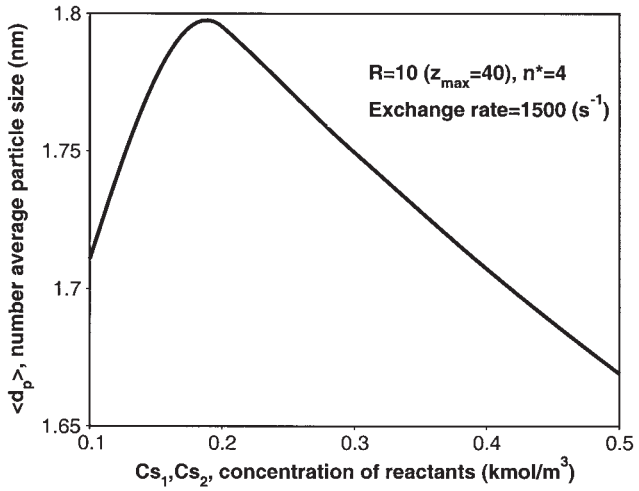

Figure 6. Effect of concentration of the reactants on the terminal particle size.

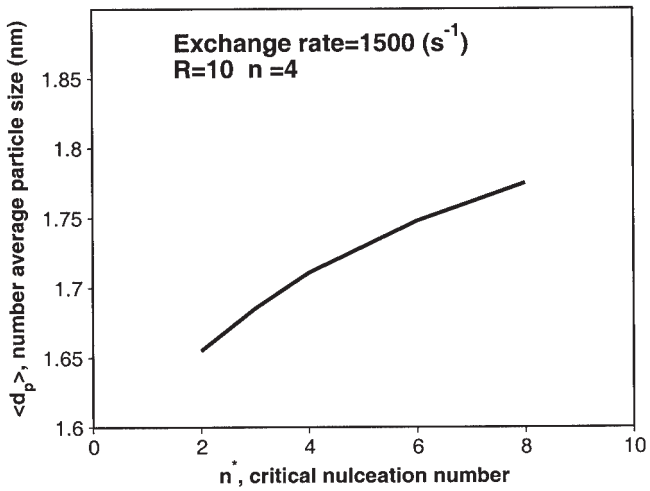

Figure 8. Effect of critical nucleation number on the terminal particle size.

size. As the concentration of reactants reaches a value where the occupancy equals, approximately, the critical nucleation number, the particle size will be maximum; further increases in concentration result in an increase in the nucleation events in micelles, leading to a decrease in the particle size.

The corresponding particle-size distribution curves are shown in Figure 7. These are similar to those obtained for $R = 10$ and 15 in Figure 5.

Effect of Critical Nucleation Number. An important parameter effecting the terminal particle size and particle-size distribution is the critical nucleation number, n^*. Figure 8 shows a monotonic increase in particle size with increasing critical nucleation number. For larger critical nucleation numbers the number of nuclei formed will be lower, giving larger particle sizes. At small values of n^*, the micelles with molecules greater than n^* will be higher, giving large number of nuclei and producing a large number of particles of small size.

The corresponding distribution curves are given in Figure 9.

Effect of Initial Reactant Ion Ratio. The effect of initial reactant ion ratio on the terminal particle size is shown in Figure 10. When the ratio is less than 1, that is $[S^{-2}]$ is less than the stoichiometric amount required for $[Cd^{+2}]$, the occupancy of $[S^{-2}]$ is lower than that of $[Cd^{+2}]$. Essentially the occupancy of $[S^{-2}]$ limits the formation of CdS. Fewer numbers of nuclei are formed, thus giving larger particle size. With increase in the ratio, the number of nuclei formed increases and thereby the terminal particle size decreases, until the other reactant becomes the limiting one.

The particle-size distributions in Figure 11 show an interesting transformation of the distribution from unimodal to bimodal when the ratio increases from 0.25 to 1 and then again to unimodal with increase in the ratio. The bimodal curve, for "ratio = 2," possibly represents an intermediate shape of the particle size distribution, between the shapes obtained for "ratio = 0.25" and "ratio = 4" (both of which are unimodal). At small values of this ratio, the number of nucleation events is restricted by the limiting reactant and these are smaller com-

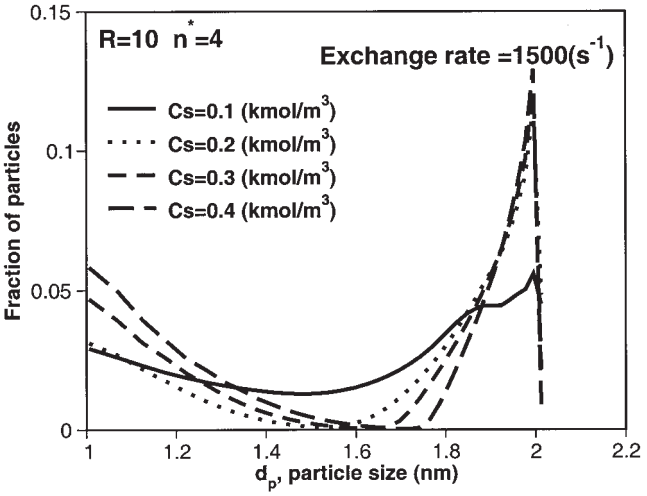

Figure 7. Effect of concentration of reactants on the particle-size distributions.

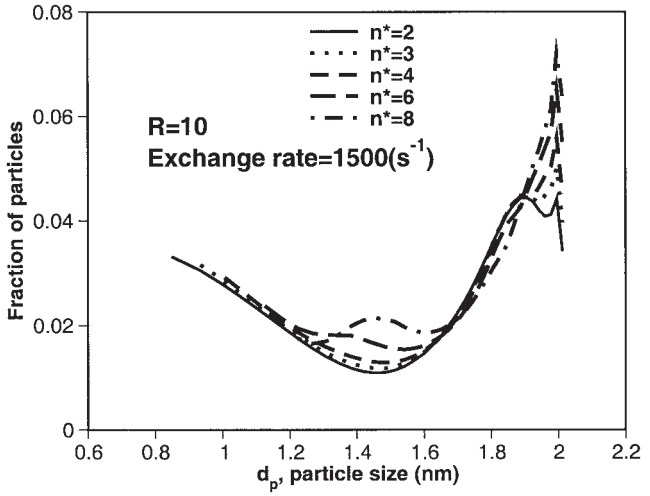

Figure 9. Effect of critical nucleation number on the particle-size distributions.

pared with the (intermicellar) exchange led growth events; at the other extreme, for large values of this ratio (which is achieved by increasing the concentration of the $[S^{-2}]$), although nucleation is still lower than growth, because of the stoichiometric limitation of the Cd ion, the absolute numbers of nucleates formed are larger than those formed in the low ratio regime. Figure 11 shows clearly that larger particles are present in greater fractions for both the ion ratios, 0.25 and 4; however, the dominant presence of larger particles is much greater for the smaller ratio. Whereas the 0.25 curve hovers close to zero and then rises sharply at higher sizes, the 4.0 curve rises almost linearly and gently, and then falls slightly, with particle size.

The possibility of bimodal distributions (or even multimodal ones) is, however, quite real in systems under consideration because of the so-called autocatalytic effect in the growth rate. This effect states that a larger particle grows faster than a smaller one because reaction/product formation occurs preferentially on the particle with greater area. We have also used this cooperative exchange rule in our study (see rule 5 in the section on Fusion–Fission Rules). A consequence of this phenomenon is that as the larger particles grow at ever greater rates, compared to smaller particles, multimodal distributions can arise when there is severe asymmetry between the number of particles that grows into a size range (slow) and those that grow out of it (rapid). Tojo et al. (1997) also reported this in their simulation studies.

Conclusions

To summarize:

(1) A model is developed based on stochastic population balance equations and a proper set of rules for intermicellar exchange, to describe formation of nanoparticles by mixing two microemulsions containing the reactants.

(2) The predictions of the model for the terminal average particle size qualitatively agree with the experimental data. The predicted size is always less than the experimentally measured size in spite of using the cooperative mode of exchange, which is likely to produce the largest particles.

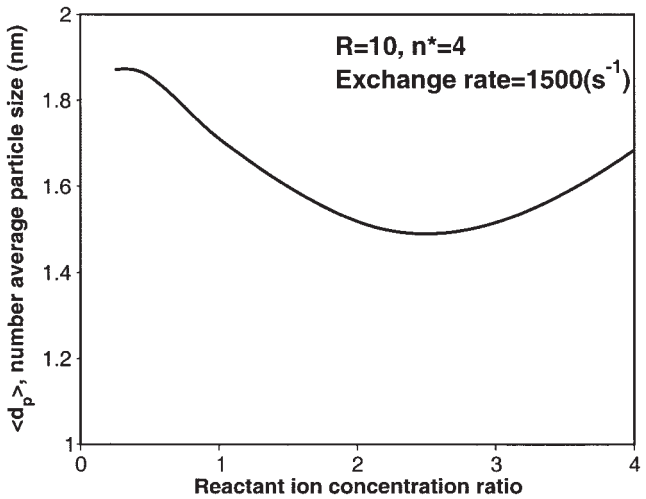

Figure 10. Effect of initial reactant ion ratio on the terminal particle size.

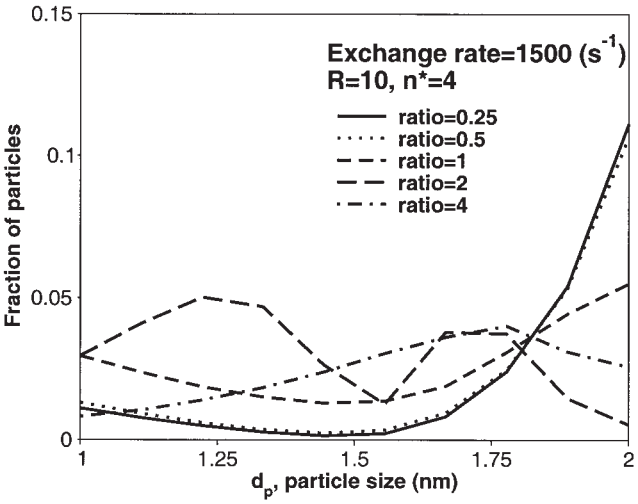

Figure 11. Effect of initial reactant ion ratio on the particle size distributions.

(3) From the model calculations it appears that nanoparticles formed by intermicellar exchange of atoms/molecules without agglomeration of any kind are a few nanometers in diameter. Formation of larger nanoparticles is most likely attributable to some additional size-enlargement processes.

Notation

A = preexponential factor of nucleation rate in micelles, s^{-1}
C_s = reactant concentration based on the aqueous phase volume, mol m^{-3}
d_p = particle size, nm
$\langle d_p \rangle$ = number-average particle size, nm
E = exchange material per unit time per unit volume, mol m^{-3} s^{-1}
e = efficiency of collisions
k_B = Boltzmann's constant = 1.38×10^{-23}, J K^{-1}
k_{ex} = second-order rate coefficient for collisional exchange, m^3 mol^{-1} s^{-1}
k_i = first-order nucleation rate in a micelle containing i number of product species, s^{-1}
M_{tot} = reverse micelles concentration based on total volume, mol m^{-3}
N_A = Avogadro's number = 6.023×10^{23}, mol^{-1}
N_{agg} = aggregation number of reverse micelle
N_b = number of micelles per unit volume, based on total volume, m^{-3}
N_p = total number of particles per unit volume, m^{-3}
n^* = critical nucleation number
q_m = Brownian collision frequency between micelles, m^3 s^{-1}
R = water-to-surfactant molar ratio
S = total surfactant concentration, based on organic phase volume, mol m^{-3}
T = temperature on absolute scale, K
V_{aq} = volume of the aqueous phase, m^3
V_{mic} = volume of the micellar core, m^3
V_{org} = volume of the organic phase, m^3
z_{avg} = average number of product species per micelle (average occupancy number)
z_{max} = maximum number of product metal atoms a reverse micelle can hold

Greek letters

α = parameter incorporating collision frequency, efficiency, and number of micelles per unit volume, referred to as collision rate, s^{-1}
η = viscosity of the continuous phase, Pa·s
λ = supersaturation in a micelle attributed to z metal atoms of any sparingly soluble salt
σ = interfacial tension between a particle and water

Literature Cited

Adamson, A., *Physical Chemistry of Surfaces*, Wiley, New York, p. 39 (1990).

Bagwe, R. P., and K. C. Khilar, "Effects of the Intermicellar Exchange Rate and Cations on the Size of Silver Chloride Nanoparticles Formed in Reverse Micelles of AOT," *Langmuir*, **13**, 6432 (1997).

Bagwe, R. P., and K. C. Khilar, "Effects of Intermicellar Exchange Rate on the Formation of Silver Nanoparticles in Reverse Microemulsions of AOT," *Langmuir*, **16**, 905 (2000).

Bandyopadhyaya, R., R. Kumar, K. S. Gandhi, and D. Ramakrishna. "Modelling of Precipitation in Reverse Micellar Systems," *Langmuir*, **13,** 3610 (1997).

Bandyopadhyaya, R., R. Kumar, K. S. Gandhi, and D. Ramakrishna. "Simulation of Precipitation Reaction in Reverse Micelles," *Langmuir*, **16,** 7139 (2000).

Barzykin, A. V., and M. Tachiya, "Generalized Model for Collisional Exchange of Solubilized Molecules in Microdisperse Systems," *Chem. Phys. Lett.*, **216**(3), 575 (1993).

Barzykin, A. V., and M. Tachiya, "Reaction Kinetics in Microdisperse Systems with Exchange," *J. Phys. Chem.*, **98**, 2677 (1994).

Boakye, E., L. R. Radovic, and K. Osseo-Asare, "Microemulsion-Mediated Synthesis of Nanosize Molybdenum Sulfide Particles," *J. Colloid Interface Sci.*, **163**, 120 (1994).

Bommarius, A. S., J. F. Holzwarth, D. I. C. Wang, and T. A., Hatton, "Coalescence and Solubilizate Exchange in a Cationic Four Component Reversed Micellar System," *J. Phys. Chem.*, **94**(18), 7232 (1994).

Chang, C., and H. Fogler, "Kinetics of Silica Particle Formation in Nonionic W/O Microemulsions from TEOS," *AIChE J.*, **42**(11), 3153 (1996).

Esquena, J., Th. F. Tadros, K. Kostarelos, and C. Solans, " Preparation of Narrow Size Distribution Silica Particles Using Microemulsions," *Langmuir*, **13**, 6400 (1997).

Fletcher, P. D. I., A. M. Howe, and B. H. Robinson, "The Kinetics of Solubilizate Exchange Between Water and Droplets of a Water-in-Oil Microemulsion," *J. Chem. Soc. Faraday Trans.*, **83**, 985 (1987).

Gleiter, H., "Nanostructured Materials: Basic Concepts and Microstructure," *Acta Mater.*, **48**, 1 (2000).

Hatton, T. A., A. S. Bommarius, and J. F. Holzwarth, "Population Dynamics of Small Systems I. Instantaneous and Irreversible Reaction in Reverse Micelles," *Langmuir*, **9**(5), 1241 (1993).

Hingorani, S., V. Pillai, P. Kumar, M. S. Multani, and D. O. Shah, "Microemulsion Mediated Synthesis of Zinc-Oxide Nanoparticles for Varistor Studies," *Mater. Res. Bull.*, **28**, 1303 (1993).

Hirai, T., H. Sato, and I. Komasawa, "Mechanism of Formation of CdS and ZnS Ultrafine Particles in Reverse Micelles," *Ind. Eng. Chem. Res.*, **33**, 3262 (1994).

Hirai, T., H. Sato, and I. Komasawa, "Mechanism of Formation of Silver Halide Ultrafine Particles in Reverse Micellar Systems," *J. Chem. Eng. Jpn.*, **29**(3), 501 (1996).

Kandori, F., K. Konno, and A. Kithara, "Formation of Ionic Water/Oil Microemulsions and Their Applications in the Preparation of Calcium Carbonate Particles," *J. Colloid Interface Sci.*, **122**, 78 (1988).

Li, Y., and C. W. Park, "Particle Size Distribution in the Synthesis of Nanoparticles Using Microemulsions," *Langmuir*, **15**(4), 952 (1999).

Lianos, P., and J. K. Thomas, "Small CdS Particles in Inverted Micelles," *J. Colloid Interface Sci.*, **117**(2), 505 (1987).

Monnoyer, Ph., A. Fonseca, and J. B. Nagy, "Preparation of Colloidal AgBr Particles from Microemulsions," *Colloids Surf. A*, **100**, 233 (1995).

Motte, L., "Synthesis *in Situ* of Nanosize Silver Sulfide Semiconductor Particles in Reverse Micelles," *J. Mater. Sci.*, **31**, 38 (1996).

Nagy, J. B., "Multinuclear NMR Characterization of Microemulsions: Preparation of Monodisperse Metal Boride Particles," *Colloids Surf. A*, **35**, 201 (1989).

Natarajan, U., K. Handique, A. Mehra, J. R. Bellare, and K. C. Khilar, "Ultrafine Metal Particle Formation in Reverse Micellar Systems: Effects of Intermicellar Exchange on the Formation of Particles," *Langmuir*, **12**, 2670 (1996).

Petit, C., P. Lixon, and M. P. Pileni, "Synthesis of CdS in Situ in Reverse Micelles. Influence of the Interface on the Growth of the Particles," *J. Phys. Chem.*, **94**, 1598 (1990).

Pileni, M. P., "Reverse Micelles as Micro-reactors," *J. Phys. Chem.*, **97**, 6961 (1993).

Pileni, M. P., "Nanosized Particles Made in Colloidal Assemblies," *Langmuir*, **13**, 3266 (1997).

Quintillan, S., C. Tojo, M. C. Blanco, and M. A. Lopez Quintela, "Effects of Intermicellar Exchange Rate on the Size Control of Nanoparticles Synthesized in Microemulsions," *Langmuir*, **17**, 7251 (2001).

Sato, H., N. Asaji, and I. Komasawa, "A Population Balance Approach for Particle Coagulation in Reverse Micelles," *Ind. Eng. Chem. Res.*, **39**, 328 (2000).

Sato, H., Y. Tsubaki, T. Hirai, and I. Komasawa, "Mechanism of Formation of Metal Sulfide Ultrafine Particles in Reverse Micelles Using Gas Injection Method," *Ind. Eng. Chem. Res.*, **96**, 92 (1997).

Suzuki, K., M. Harada, and A. Shioi, "Growth Mechanism of CdS Ultrafine Particles in Water in Oil Microemulsions," *J. Chem. Eng. Jpn.*, **29**, 264 (1996).

Tojo, C., "Preparation of Nanoparticles in Microemulsions: A Monte Carlo Study of the Influence of the Synthesis Variables," *Langmuir*, **13**, 4527 (1997).

Towey, T. F., A. K. Lodhi, and B. H. Robinson, "Kinetics and Mechanism of Formation of Quantum Sized CdS Particles inWater–Aerosol OT–Oil Microemulsions," *J. Chem. Soc. Faraday Trans.*, **86**(22), 3757 (1990).

Ueda, M., and Z. A. Schelly, " Mean Aggregation Number and Water Vapor Pressure of AOT Reverse Micellar Systems Determined by Controlled Partial Pressure-Vapor Pressure Osmometry (CPP-VPO)," *Langmuir*, **4**, 653 (1988).

Wang, G. H., and G. L. Li, "Synthesis of Nanometer Sized TiO_2 Particles by Microemulsion Method," *Nanostruct. Mater.*, **11**(5), 663 (1999).

Appendix

$$\frac{dpa(i)}{dt} = -\alpha \times pa(i)\{\sum_{j=1}^{z_{\max}-i} pa(j) + \sum_{j=1}^{z_{\max}} pb(j) + \sum_{j=1}^{z_{\max}-i-1}\sum_{k=0}^{z_{\max}-i-j} (pza(j)(k) + ppa(j)(k)) + \sum_{j=1}^{z_{\max}-i}\sum_{k=0}^{z_{\max}} (pzb(j)(k) + ppb(j)(k))\} + \frac{1}{2}\alpha\sum_{j=1}^{i-1} pa(j) \times pa(i-j) \quad \text{(A1)}$$

Conditions for above equation: For 5th and 6th terms $(j + k) < z_{\max}$

$$\frac{dpb(i)}{dt} = -\alpha \times pb(i)\left\{\sum_{j=1}^{z_{\max}-i} pb(j) + \sum_{j=1}^{z_{\max}} pa(i) + \sum_{j=1}^{z_{\max}-i}\sum_{k=1}^{z_{\max}} (pza(j)(k) + ppa(j)(k)) + \sum_{j=1}^{z_{\max}-i-1}\sum_{k=1}^{z_{\max}-i-j} (pzb(j)(k) + ppb(j)(k))\right\} + \frac{1}{2}\alpha\sum_{j=1}^{i-1} pb(j) \times pb(i-j) \quad \text{(A2)}$$

Conditions for above equation: For 5th and 6th terms $(j + k) < z_{\max}$

$$\frac{dpza(i)(j)}{dt} = -k_i \times pza(i)(j) - \alpha \times pza(i)(j)\left\{\sum_{k=1}^{z_{max}-i-j} pa(k) + \sum_{k=1}^{z_{max}} pb(k) + \frac{1}{2}\sum_{k=1}^{z_{max}-i-j-1}\sum_{l=0}^{z_{max}-i-j-k} pza(k)(l) + \sum_{k=1}^{z_{max}-i-j-1}\sum_{l=0}^{z_{max}} pzb(k)(l) + \sum_{k=1}^{z_{max}-i-j-1}\sum_{l=0}^{z_{max}-i-j-k} ppa(k)(l) + \sum_{k=1}^{z_{max}-i-j-1}\sum_{l=0}^{z_{max}} ppb(k)(l)\right\} + \alpha \sum_{k=1}^{i-1} pzb(k)(i-k) \times pa(i-k+j)$$
$$+ \alpha \sum_{k=1}^{i-1}\sum_{l=0}^{i-k-1} pza(k)(l+j) \times pzb(i-k-l)(l) + \frac{1}{2}\alpha \sum_{k=1}^{i-1}\sum_{l=0}^{j-1} pza(k)(l) \times pza(i-k)(j-l) + \alpha \sum_{k=1}^{j-1} pza(i)(k) \times pa(j-k)$$
$$+ \alpha \sum_{k=1}^{i-1} pza(k)(i-k+j) \times pb(i-k) + \alpha \times pa(i+j) \times pb(i) \quad \text{(A3)}$$

Conditions for the above equation: 1st term: $i > n^*$, 3rd term: $(i + k) < z_{max}$, 5th and 7th terms: $(i + k + j) < z_{max}$, 9th term: $(l + j) < z_{max}$, 10th term: $(i - k + j) < z_{max}$

$$\frac{dpzb(i)(j)}{dt} = -k_i \times pzb(i)(j) - \alpha \times pzb(i)(j)\left\{\sum_{k=1}^{z_{max}-i-j} pb(k) + \sum_{k=1}^{z_{max}} pa(k) + \frac{1}{2}\sum_{k=1}^{z_{max}-i-j-1}\sum_{l=0}^{z_{max}-i-j-k} pzb(k)(l) + \sum_{k=1}^{z_{max}-i-j-1}\sum_{l=0}^{z_{max}} pza(k)(l) + \sum_{k=1}^{z_{max}-i-j-1}\sum_{l=0}^{z_{max}-i-j-k} ppb(k)(l) + \sum_{k=1}^{z_{max}-i-j-1}\sum_{l=0}^{z_{max}} ppa(k)(l)\right\} + \alpha \sum_{k=1}^{i-1} pza(k)(i-k) \times pb(i-k+j)$$
$$+ \alpha \sum_{k=1}^{i-1}\sum_{l=0}^{i-k-1} pzb(k)(l+j) \times pza(i-k-l)(l) + \frac{1}{2}\alpha \sum_{k=1}^{i-1}\sum_{l=0}^{j-1} pzb(k)(l) \times pzb(i-k)(j-l) + \alpha \sum_{k=1}^{j-1} pzb(i)(k) \times pb(j-k)$$
$$+ \alpha \sum_{k=1}^{i-1} pzb(k)(i-k+j) \times pa(i-k) + \alpha \times pa(i) \times pb(i+j) \quad \text{(A4)}$$

Conditions for the above equation: 1st term: $i > n^*$, 3rd term: $(i + k) < z_{max}$, 5th and 7th terms: $(i + k + j) < z_{max}$, 9th term: $(l + j) < z_{max}$, 10th term: $(i - k + j) < z_{max}$

$$\frac{dppa(i)(j)}{dt} = k_i \times pza(i)(j) - \alpha \times ppa(i)(j)\{\sum_{k=1}^{z_{max}-i-j} pa(k) + \sum_{k=1}^{z_{max}} pb(k) + \sum_{k=1}^{z_{max}-i-j-1}\sum_{l=0}^{z_{max}-i-j-k} pza(k)(l) + \sum_{k=1}^{z_{max}-i-j}\sum_{l=0}^{z_{max}} pzb(k)(l)$$
$$+ \sum_{k=1}^{z_{max}}\sum_{l=0}^{z_{max}} ppa(k)(l) + \sum_{k=1}^{z_{max}}\sum_{l=0}^{z_{max}} ppb(k)(l)\} + \alpha \sum_{k=1}^{i-1}(ppa(k)(i-k+j)pb(i-k) + ppb(k)(i-k) \times pa(i-k+j)) + \alpha \sum_{k=0}^{j-1} ppa(i)(k)$$
$$\times pa(j-k) + \alpha \sum_{k=1}^{i-1}\sum_{l=0}^{j-1} ppa(k)(l) \times pza(i-k)(j-l) + \alpha \sum_{k=1}^{i-1}\sum_{l=0}^{i-k} ppa(k)(l) \times pzb(i-k-l)(j-l) + \alpha \sum_{k=1}^{i-1}\sum_{l=0}^{i-k} ppb(k)(l)pza(i-k$$
$$- l)(j+l) + \alpha \sum_{k=1}^{z_{max}}\sum_{l=0}^{j-1} ppa(i)(j) \times ppa(k)(j-l) + \alpha \sum_{k=1}^{i-1}\sum_{l=0}^{j-1} \text{if } (k >= l) \text{ then } ppa(k)(i+j-k) \times ppb(l)(i-k) \text{ else } ppa(k)(i+j$$
$$- l) \times ppb(l)(i-l) \quad \text{(A5)}$$

Conditions for the above equation: 1st term: $i > n^*$, 3rd term: $(i + k) < z_{max}$, 5th term: $(i + k + j) < z_{max}$, 6th term: if $(i > k)$ then $(i + j + l) < z_{max}$ else $(k + j + l) <= z_{max}$, 7th term: if $(i >= k)$ and if $(j <= l)(i + l) <= z_{max}$ else $(i + j) <= z_{max}$ else if $(j <= l)(k + l) <= z_{max}$ else $(k + j) <= z_{max}$, 9th term: $(l + j) < z_{max}$, 10th term: $(i - k + j) < z_{max}$, 12th term: $(j + l) < z_{max}$

$$\frac{dppb(i)(j)}{dt} = k_i \times pzb(i)(j) - \alpha \times ppb(i)(j)\{\sum_{k=1}^{z_{max}-i-j} pb(k) + \sum_{k=1}^{z_{max}} pa(k) + \sum_{k=1}^{z_{max}-i-j-1}\sum_{l=0}^{z_{max}-i-j-k} pzb(k)(l) + \sum_{k=1}^{z_{max}-i-j-1}\sum_{l=0}^{z_{max}} pza(k)(l)$$

$$+ \sum_{k=1}^{z_{max}}\sum_{l=0}^{z_{max}} ppa(k)(l) + \sum_{k=1}^{z_{max}}\sum_{l=0}^{z_{max}} ppb(k)(l)\} + \alpha \sum_{k=1}^{i-1} (ppb(k)(i-k+j) \times pa(i-k)$$

$$+ ppa(k)(i-k) \times pb(i-k+j)) + \alpha \sum_{k=1}^{j-1} ppb(i)(k) \times pb(j-k) + \alpha \sum_{k=1}^{i-1}\sum_{l=0}^{j-1} ppb(k)(l) \times pzb(i-k)(j-l) + \alpha \sum_{k=1}^{z_{max}}\sum_{l=0}^{j-1} ppb(i)(j)$$

$$\times ppb(k)(j-l) + \alpha \sum_{k=1}^{i-1}\sum_{l=0}^{i-k} ppb(k)(l) \times pza(i-k-l)(j-1) + \alpha \sum_{k=1}^{z_{max}}\sum_{l=0}^{j-1} ppb(k)(i+j-k) \times ppa(l)(i-k) + \alpha \sum_{k=1}^{i-1}\sum_{l=0}^{j-1} \text{if } (k$$

$$>= l) \text{ then } ppb(k)(i+j-k) \times ppa(l)(i-k) \text{ else } ppb(k)(i+j-l) \times ppa(l)(i-l) \quad \text{(A6)}$$

Conditions for the above equation: 1st term: $i > n^*$, 3rd term: $(i + k) < z_{max}$, 5th term: $(i + k + j) < z_{max}$, 6th term: if $(i >= k)$ and if $(j <= l)(i + l) <= z_{max}$ else $(i + j) <= z_{max}$ else if $(j <= l)(k + l) <= z_{max}$ else $(k + j) <= z_{max}$, 7th term: if $(i > k)$ then $(i + j + l) < z_{max}$ else $(k + j + l) <= z_{max}$, 9th term: $(l + j) < z_{max}$, 10th term: $(i - k + j) < z_{max}$, 14th term: $(j + l) < z_{max}$.

Manuscript received Feb. 22, 2003, and revision received Sep. 23, 2003.